

Glucuronidation of Psilocin and 4-Hydroxyindole by the Human UDP-Glucuronosyltransferases

Nenad Manevski, Mika Kurkela, Camilla Höglund, Timo Mauriala, Michael H. Court, Jari Yli-Kauhaluoma, and Moshe Finel

Division of Pharmaceutical Chemistry (N.M., J.Y.-K.), and Centre for Drug Research (M.K., C.H., T.M., M.F.), Faculty of Pharmacy, University of Helsinki, Helsinki, Finland; and Department of Pharmacology and Experimental Therapeutics, Tufts University School of Medicine, Boston, Massachusetts (M.H.C.)

Received November 10, 2009; accepted December 10, 2009

ABSTRACT:

We have examined the glucuronidation of psilocin, a hallucinogenic indole alkaloid, by the 19 recombinant human UDP-glucuronosyltransferases (UGTs) of subfamilies 1A, 2A, and 2B. The glucuronidation of 4-hydroxyindole, a related indole that lacks the *N,N*-dimethylaminoethyl side chain, was studied as well. UGT1A10 exhibited the highest psilocin glucuronidation activity, whereas the activities of UGTs 1A9, 1A8, 1A7, and 1A6 were significantly lower. On the other hand, UGT1A6 was by far the most active enzyme mediating 4-hydroxyindole glucuronidation, whereas the activities of UGTs 1A7–1A10 toward 4-hydroxyindole resembled their respective psilocin glucuronidation rates. Psilocin glucuronidation by UGT1A10 followed Michaelis-Menten kinetics in which psilocin is a low-affinity high-turnover substrate ($K_m = 3.8$ mM; $V_{max} = 2.5$ nmol/min/mg). The kinetics of psilocin glucuronidation by UGT1A9

was more complex and may be best described by biphasic kinetics with both intermediate ($K_{m1} = 1.0$ mM) and very low affinity components. The glucuronidation of 4-hydroxyindole by UGT1A6 exhibited higher affinity ($K_m = 178$ μ M) and strong substrate inhibition. Experiments with human liver and intestinal microsomes (HLM and HIM, respectively) revealed similar psilocin glucuronidation activity in both samples, but a much higher 4-hydroxyindole glucuronidation rate was found in HLM versus HIM. The expression levels of UGTs 1A6–1A10 in different tissues were studied by quantitative real-time-PCR, and the results, together with the activity assays findings, suggest that whereas psilocin may be subjected to extensive glucuronidation by UGT1A10 in the small intestine, UGT1A9 is likely the main contributor to its glucuronidation once it has been absorbed into the circulation.

Psilocybin and its dephosphorylated active metabolite, psilocin, are hallucinogenic indole alkaloids that are found around the world in numerous species of the genus *Psilocybe* mushrooms, commonly referred to as “magic mushrooms” (Stamets, 2003). The possession, cultivation, and intake of mushrooms containing psilocybin and psilocin are prohibited in most countries, but they are nevertheless used as recreational drugs (Tsuji-kawa et al., 2003; Halpern, 2004; Bjornstad et al., 2009). After administration, psilocybin is rapidly dephosphorylated to its active metabolite, psilocin (Hasler et al., 1997 and references therein) (Fig. 1), which acts as an agonist of serotonin presynaptic 5-hydroxytryptamine_{2A} receptors (Gonzalez-Maeso et al., 2007).

Early metabolic studies suggested that psilocin only undergoes oxidative metabolism via a presumed intermediate metabolite, 4-hydroxyindole-3-acetaldehyde, to yield 4-hydroxyindole-3-acetic acid

This work was supported in part by the National Institutes of Health National Institute of General Medical Sciences [Grant GM061834] (to M.H.C.); the Academy of Finland [Grant 120975] (to J.Y.-K.); the Research Foundation of the University of Helsinki (to N.M.); and the Sigrid Juselius Foundation (to M.F.).

Article, publication date, and citation information can be found at <http://dmd.aspetjournals.org>.

doi:10.1124/dmd.109.031138.

and 4-hydroxytryptophole (Holzmann, 1995; Hasler et al., 1997). However, later pharmacokinetic and forensic studies provided evidence that psilocin is mostly eliminated by conjugative metabolism as psilocin glucuronide (Sticht and Käferstein, 2000; Grieshaber et al., 2001). It was found that addition of β -glucuronidase to the detection assays for psilocin in body fluids yielded additional psilocin, presumably released from psilocin glucuronide (Hasler et al., 2002; Kamata et al., 2003). Moreover, direct analysis by liquid chromatography-mass spectrometry (LC-MS) of serum samples 5 h after mushroom intoxication showed that up to 80% of the psilocin was present as the glucuronide conjugate (Kamata et al., 2006).

The 4-hydroxyindole was included in this study because it is structurally closely related to psilocin, as well as to the neurotransmitter serotonin (5-hydroxytryptamine), but lacks the conformationally flexible side chain found in both of them (Fig. 1). Although no report on the glucuronidation of 4-hydroxyindole has been published so far, it may prove to be an interesting compound for studies of human UDP-glucuronosyltransferases (UGTs) substrate selectivity. Many bioactive compounds of either endogenous origin, like serotonin and melatonin, or drugs such as indomethacin, ondansetron, tadalafil, frovatriptan, and various tryptamines, include an indole scaffold.

ABBREVIATIONS: LC-MS, liquid chromatography-mass spectrometry; UGT, UDP-glucuronosyltransferase; UDPGA, UDP- α -D-glucuronic acid; HLM, human liver microsomes; CAS, Chemical Abstract Service; DTT, DL-dithiothreitol; HPLC, high-performance liquid chromatography; HIM, human intestinal microsomes; UPLC, ultraperformance liquid chromatography; DMSO, dimethyl sulfoxide; qRT-PCR, quantitative real-time PCR.

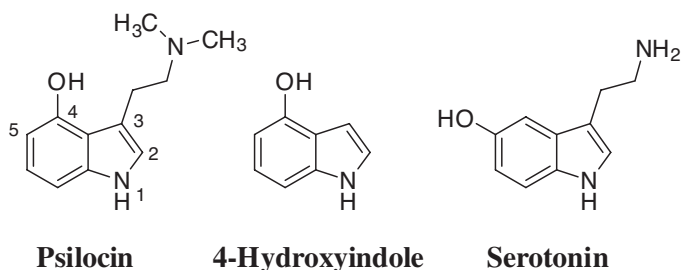


FIG. 1. Chemical structures of psilocin, 4-hydroxyindole, and serotonin.

The UGTs are membrane proteins of the endoplasmic reticulum that catalyze the transfer of glucuronic acid from UDP- α -D-glucuronic acid (UDPGA) to various endogenous and xenobiotic compounds bearing different nucleophilic groups, thereby increasing aqueous solubility and facilitating their excretion from the body (King et al., 2000; Tukey and Strassburg, 2000). The 19 known functional human UGTs are categorized into three subfamilies, 1A, 2A, and 2B, based on gene structure and sequence homology (Mackenzie et al., 2005). The UGTs are variably expressed in different tissues, such as liver, gastrointestinal tract, kidneys, and others (Turgeon et al., 2001; Mackenzie et al., 2005; Nakamura et al., 2008; Ohno and Nakajin, 2009). Most UGTs have broad and partly overlapping substrate selectivity, although often with different kinetic parameters for the same reactions (Itäaho et al., 2008; Kaivosari et al., 2008). In addition, a majority of human tissues that express a UGT, express more than one UGT enzyme. Thus, using native samples such as human liver microsomes (HLM) is rarely suitable for reliable identification of specific UGTs, mediating a particular reaction and individual recombinant enzymes are better study materials for such investigations.

As far as we know, the glucuronidation of psilocin by individual human UGTs has not been examined before. Studies of the structurally close and pharmacologically related compound, the neurotransmitter serotonin, revealed that it is glucuronidated almost exclusively by UGT1A6 (Krishnaswamy et al., 2003; Kurkela et al., 2007). The main aims of this study were to identify the UGTs that catalyze psilocin and 4-hydroxyindole glucuronidation, to characterize the kinetics of these reactions, and to locate the tissues where the activities are likely to take place. Special attention was given to the chemical stability of psilocin and possible ways to increase it during the *in vitro* incubations. The results provide interesting new insight into the substrate selectivity of the human UGTs.

Materials and Methods

Materials. 4-Hydroxyindole [$>99.0\%$, Chemical Abstract Service (CAS) number 2380-94-1] was acquired from TCI Europe (Zwijndrecht, Belgium), UDPGA (triammonium salt, 98–100%, CAS number 63700-19-6), DL-dithiothreitol [(DTT) $\geq 99.5\%$, CAS number 3483-12-3], alamethicin ($>90\%$, CAS number 27061-78-5), β -estradiol ($\geq 98\%$, CAS number 50-28-2), and 1-naphthol (99%, CAS number 90-15-3) were purchased from Sigma-Aldrich (St. Louis, MO). Radiolabeled [^{14}C]UDPGA was acquired from PerkinElmer Life and Analytical Sciences (Waltham, MA). Magnesium chloride hexahydrate and perchloric acid were obtained from Merck (Darmstadt, Germany). Formic acid (98–100%) was obtained from Riedel-de Haën (Seelze, Germany). High-performance liquid chromatography (HPLC)-grade solvents were used throughout the study.

Psilocin Preparation. Psilocin (4-hydroxy-*N,N*-dimethyltryptamine, as a free base) was synthesized from 4-hydroxyindole as described previously (Shirota et al., 2003), with permission from the National Agency for Medicines (01/2008, Helsinki, Finland). The crude product was purified on a Biotage Sp1 automated purification system (Biotage, Uppsala, Sweden) equipped with flash 12+M silica cartridges and UV detection at 254 nm. The mobile phase contained chloroform (A) and methanol (B). A gradient elution was applied,

10 \rightarrow 20% B during 10 column volumes. Purified fractions were combined and organic solvents were evaporated *in vacuo* to yield white solids. Purity was assessed as $>98\%$ by ^1H NMR and LC-UV/MS analyses. Solid product was kept in a dark vial at -20°C under argon.

Enzyme Sources. Recombinant human UGTs were expressed as His-tagged proteins in baculovirus-infected Sf9 insect cells as described previously (Kurkela et al., 2007 and references therein). The human UGTs of subfamily UGT2A were expressed in a similar way (Sneitz et al., 2009). The relative expression level of each recombinant UGT isoform was immunodetected by using tetra-His antibodies (QIAGEN, Hilden, Germany) as described earlier (Kurkela et al., 2007). Protein concentrations were determined by the BCA method (Pierce Biotechnology, Rockford, IL). Pooled HLM (lot 70196), human intestinal microsomes [(HIM) lot 15031], and commercial recombinant human UGT2B15 expressed in insect cells were purchased from BD Gentest (Woburn, MA).

Psilocin and 4-Hydroxyindole Glucuronidation Assays. Stock solutions of psilocin and 4-hydroxyindole, 100 mM in methanol, were diluted with methanol to the desired concentrations immediately before use. Aliquots of these dilutions were transferred to 1.5-ml centrifuge tubes, and the solvent was evaporated *in vacuo* at ambient temperature. The solid residues were dissolved in the reaction mixture to yield the desired substrate concentration. The reaction mixture consisted of phosphate buffer (50 mM, pH 7.4), MgCl_2 (10 mM), DTT (1 mM, for psilocin samples only), and protein (0.05–1.5 mg/ml, depending on the enzyme source) in a final volume of 100 μl , unless otherwise stated. The suspension was incubated first for 30 min at room temperature, followed by 5-min incubation at 37°C . The glucuronidation reactions were initiated by the addition of UDPGA to a final concentration of 5 mM and carried out at 37°C , protected from light. The reactions were terminated by the addition of 10 μl of ice-cold 4 M perchloric acid. In some cases, the reactions were terminated by the addition of equal volume of cold methanol (-20°C) rather than perchloric acid addition. After termination, the tubes were transferred to ice for 30 min and then centrifuged at 16000g for 10 min. Aliquots of the resulting supernatants were transferred to dark glass vials and subjected to either HPLC, ultraperformance liquid chromatography (UPLC), or LC-MS analyses.

Analytical Methods. The HPLC system consisted of the Agilent 1100 series degasser, binary pump, autosampler, thermostated column compartment, multiple wavelength UV detector, and fluorescence detector (Agilent Technologies, Palo Alto, CA). This system was connected to a 9701 HPLC radioactivity monitor (Reeve Analytical, Glasgow, Scotland). The resulting chromatograms were analyzed with Agilent ChemStation software (revision B.01.01) on Windows 2000 Professional workstation.

We have developed two HPLC methods to separate psilocin glucuronides, using UV absorbance detection at 270 nm in both cases. In method A, the column was Agilent Zorbax Eclipse C18 Plus (250 \times 4.6 mm, 5 μm ; Agilent Technologies) and the column temperature was 40°C . The mobile phase consisted of 0.1% formic acid (A, aqueous) and methanol (B), and the gradient elution was as follows: 0 to 5 min of 5% B and a flow rate of 1.0 ml/min; 5 to 17 min of 5 \rightarrow 40% B at 1 ml/min; and 17 to 25 min of 5% B again, but at a flow rate of 1.5 ml/min. The retention time of the psilocin glucuronide in method A was 11.4 min.

In method B for psilocin glucuronide, the column was Supelco Discovery HS F5 (4 \times 150 mm, 3 μm ; Supelco, Bellefonte, PA), column temperature 40°C . The mobile phase consisted of 0.1% formic acid (A) and acetonitrile (B), and the flow rate was 0.8 ml/min throughout. The gradient in this method was as follows: 0 to 5 min of 5% B; 5 to 15 min of 5 to 50% B; and 15 to 25 min of 5% B again. The psilocin glucuronide retention time in method B was 5.9 min.

The 4-hydroxyindole glucuronide was detected using method A that is described above for psilocin glucuronide separation and detection. The retention time of 4-hydroxyindole-glucuronide in this method was 12.6 min. Estradiol-3-glucuronide was detected by HPLC as described previously (Itäaho et al., 2008).

The UPLC system was Waters Acquity UPLC (Waters, Milford, MA) equipped with column manager, sample manager, binary solvent pump, and photodiode array UV detector. The resulting chromatograms were analyzed with Empower 2 software (Build 2154; Waters) on Windows XP Professional. We have developed a UPLC method to separate 4-hydroxyindole glucuronide in the presence of psilocin or 1-naphthol and the corresponding glucuronide

conjugates. The UPLC column was Acquity UPLC BEH C₁₈ (1.7 μ m, 2.1 \times 100 mm; Waters), equipped with a precolumn, and the column temperature was 40°C. The mobile phase consisted of 0.1% formic acid (A) and acetonitrile (B), and the flow rate was 0.6 ml/min throughout. UV absorbance at 262 nm was used for detection. The gradient in this method was as follows: 0 to 4 min of 2 \rightarrow 4% B; 4 to 4.5 min of 4 \rightarrow 85% B; 4.5 to 5 min of 85 \rightarrow 2% B; and 5 to 7 min of 2% B. The 4-hydroxyindole glucuronide retention time in this method was 2.35 min.

Mass spectrometry data were acquired with Agilent 6410 Triple Quadrupole instrument (Agilent Technologies) using electrospray ionization at positive ion mode. Nitrogen was used both as the nebulizer (35 psi) and the curtain gas (350°C, 10 l/min). The capillary voltage was 4000 V. The LC-MS analyses were carried out by using MS scan mode (scan range, m/z 100–650; fragmentor voltage, 85 V) and selected ion monitoring mode for the precursor ions m/z 381 (psilocin glucuronide) and m/z 310 (4-hydroxyindole glucuronide). The fragmentor voltage was 85 V and the collision energy was 20 eV. MS data were collected and processed by Agilent MassHunter - Qualitative Analysis software (version B.01.03) on Windows XP Professional.

Glucuronide Quantification. Psilocin and 4-hydroxyindole glucuronides were quantified by using a combination of radiochemical and UV detection, except in the case of UPLC where the quantification was performed based on the standard curve made by using the aglycone, 4-hydroxyindole. In the combined radioactive-UV analysis of psilocin, a glucuronidation reaction containing 1.5 mg/ml recombinant UGT1A10 in a final volume of 360 μ l was carried out in the presence of 1 mM psilocin. The cosubstrate mixture in this case contained 15.4 μ M radiolabeled [¹⁴C]UDPGA and 500 μ M unlabeled UDPGA, and the incubation time was 120 min at 37°C. After termination and centrifugation, eight aliquots of the supernatant, ranging in volume from 1 to 80 μ l, were injected into the HPLC system equipped with both radiochemical and UV-diode array detector detectors. The amount of formed glucuronide (x , nmol) was calculated based on the radiochemical detector signals and the following equation:

$$x = A \frac{B}{B + C}$$

where A is the total amount of UDPGA in the injection volume (nmol), B is the area of the psilocin glucuronide peak, and C is the area of the free UDPGA peak. The calculated amounts of psilocin glucuronide were plotted against the area of the corresponding peaks in the UV chromatogram, and the resulting plot was fitted by linear regression to yield a standard curve with excellent linearity ($r^2 > 0.997$). The standard curve for 4-hydroxyindole glucuronide was determined in the similar fashion, except that the enzyme was UGT1A6. The linearity of the 4-hydroxyindole glucuronide standard curve was also very good ($r^2 > 0.994$). The standard curve for 4-hydroxyindole glucuronide in the UPLC system was generated by using 4-hydroxyindole as a standard, assuming that the UV absorbance of 4-hydroxyindole and its glucuronide are similar.

Effect of DTT on Psilocin Glucuronidation and Product Stability. The effect of DTT on the stability of psilocin and its glucuronide was determined by adding this reducing agent to two different reactions catalyzed by UGT1A10, psilocin glucuronidation and β -estradiol glucuronidation. The reactions were performed in the presence of either 1 mg/ml UGT1A10 and 1 mM psilocin, or 0.2 mg/ml UGT1A10 and 100 μ M estradiol. The DTT concentrations in the assays were 0, 0.5, 1.0, 2.5, 5.0, or 10 mM. The β -estradiol glucuronidation reaction mixture also contained 5% dimethyl sulfoxide (DMSO). The reaction time, at 37°C, was either 30 min for β -estradiol or 60 min for psilocin. For assessing the stability of psilocin glucuronide under the supernatant conditions after reaction termination and centrifugation, the glucuronidation reaction with UGT1A10 was carried out as described, except that the volume was increased to 500 μ l. After reaction termination by the addition of 50 μ l of perchloric acid (4 M) and the subsequent sample processing, aliquots were transferred to dark glass vials and placed on the autosampler plate at room temperature and analyzed by HPLC at 8-h intervals over a 72-h period.

Screening of HLM, HIM, and Recombinant UGTs. Psilocin glucuronidation by the different samples was carried out at three substrate concentrations, 100, 500, and 1000 μ M. The corresponding screens for 4-hydroxyindole glucuronidation were carried out at two substrate concentrations (100 and 500

μ M). The protein concentrations of recombinant UGTs, HLM, and HIM in screening assays were 0.50, 0.25, and 0.50 mg/ml, respectively. The latter two sets of reactions also contained alamethicin at a final concentration of 5% of the microsomal protein concentrations. The reaction tubes that contained alamethicin were placed on ice for 30 min before moving on to the glucuronidation assays (Fisher et al., 2000). Incubation time varied from 60 to 120 min. Glucuronidation activities are reported as the average and S.E. of at least three replicate determinations. The glucuronidation rates by recombinant enzymes are also reported as “normalized” values. In this case the reaction rate was divided by the relative expression level of the given recombinant UGT. The relative expression level of each recombinant UGT was measured by immunoblotting as described previously (Kurkela et al., 2007) and setting the expression level of UGT1A10 at 1.0 for this set of experiments.

Enzyme Kinetic Analysis. The protein concentrations and incubation times for the kinetic analyses reactions were selected based on preliminary assays to ensure that product formation was within the linear range with respect to protein concentration and time and that the substrate consumption was less than 10%. Psilocin kinetics with UGT1A9 (0.20 mg/ml, 60-min incubation) and UGT1A10 (0.25 mg/ml, 60-min incubation) were studied at 12 substrate concentrations, ranging from 50 to 5000 μ M. Glucuronidation kinetic analysis of 4-hydroxyindole with UGT1A6 (0.05 mg/ml, 20-min incubation) contained 8 substrate concentrations, ranging from 25 to 5000 μ M, whereas UGT1A10 was assayed for 4-hydroxyindole glucuronidation kinetics under the same conditions as those for psilocin glucuronidation (see above). The kinetics of 4-hydroxyindole glucuronidation by UGT2A1 was carried out essentially as that for UGT1A10, except that the incubation time was 30 min.

Enzyme kinetic parameters were obtained by fitting kinetic models to experimental data by using GraphPad Prism version 5.01 for Windows (GraphPad Software Inc., San Diego, CA). The best model was selected based on the corrected Akaike's information criterion, the calculated r^2 values, residuals graph, parameter S.E. estimates, 95% confidence intervals, and visual inspection of Eadie-Hofstee plots. Data were fitted with the following four models:

1. Michaelis-Menten equation:

$$v = \frac{V_{\max}[S]}{K_m + [S]}$$

where v is the initial velocity of the enzyme reaction, V_{\max} is the maximum velocity, $[S]$ is the substrate concentration, and K_m is the velocity at 0.5 of V_{\max} .

2. Substrate inhibition model equation:

$$v = \frac{V_{\max}[S]}{K_m + [S] \left(1 + \frac{[S]}{K_i} \right)}$$

where K_i is the constant describing the substrate inhibition interaction.

3. Allosteric sigmoidal model (Hill equation):

$$v = \frac{V_{\max}[S]^h}{S_{50}^h + [S]^h}$$

where S_{50} is the velocity at 0.5 of V_{\max} (analogous to K_m in Michaelis-Menten model), and h is the Hill coefficient.

4. Two-site biphasic model equation (Korzekwa et al., 1998):

$$v = \frac{V_{\max 1}[S] + CL_{\text{int}}[S]^2}{K_{m1} + [S]}$$

where $V_{\max 1}$ and K_{m1} are estimated from the curved portion of the plot at lower substrate concentrations. The CL_{int} represents the ratio of $V_{\max 2}/K_{m2}$ and describes the linear portion of the plot exhibited at higher substrate concentrations.

Inhibition of 4-Hydroxyindole Glucuronidation by UGT1A6 in the Presence of Psilocin and 1-Naphthol. Inhibition of 4-hydroxyindole glucuronidation by UGT1A6 (0.05 mg/ml) was assessed in the presence of 200 μ M substrate and different concentrations of either psilocin (0–3000 μ M) or 1-naphthol (0–200 μ M). DTT was included in all of these samples. The incubation time was 30 min. Results are presented as percentage of the remaining activity, relative to control incubations without the tested inhibitor.

Real-Time Quantitative PCR of UGTs in Human Tissues. Results of quantitation of UGT1A9 and UGT1A10 mRNA in human tissues have been reported previously (Itäaho et al., 2009). For this study, expression of other UGT isoforms found to be active against psilocin and 4-hydroxyindole (including UGT1A6, UGT1A7, and UGT1A8) were measured in the same samples as follows. Total RNA extracted from 47 human livers was pooled. Liver donors were all of European-American ancestry and included both males ($n = 36$) and females ($n = 11$). Use of the tissue was approved by the institutional review board of Tufts University School of Medicine. Total RNA purchased from Clontech (Mountain View, CA) included human adrenal gland ($n = 62$), whole brain, cerebellum ($n = 24$), fetal brain ($n = 59$), colon ($n = 3$), kidney, lung, placenta, prostate ($n = 47$), small intestine ($n = 5$), testis ($n = 19$), thyroid ($n = 65$), trachea, and uterus ($n = 10$), whereas total RNA from Ambion (Austin, TX) included human adipose tissue, stomach, pancreas, and ovary. Total RNA ($1 \mu\text{g}$) was treated with DNase (Promega, Madison, WI) and cDNA synthesized by reverse transcription (Superscript II; Invitrogen, Carlsbad, CA) with random hexamer primer ($0.1 \mu\text{g}$). Quantitative PCR reactions ($25 \mu\text{l}$) included SYBR Green 2 \times master mix (Applied Biosystems, Foster City, CA), $10 \mu\text{l}$ of 1:10 diluted cDNA (except 1:30 dilution for liver cDNA; and 1:500 dilution for cDNA assayed with 18S rRNA primers), and 100 nM of each primer (200 nM for 18S RNA). Primer pair sequences were as follows: CCC CTC GAT GCT CTT AGC TGA GTG T (18S-rRNA-forward) and CGC CGG TCC AAG AAT TTC ACC TCT (18S-rRNA-reverse); GTT TTC CGT GTT CCC TGG AGC (UGT1A6-forward) and CCA ACA AAT TAA CAA GGA AGT TGG C (UGT1A6-reverse); GCC GAT GCT CGC TGG ACG (UGT1A7-forward) and AGG ATC GAG AAA CAC TGC ATC AAA AC (UGT1A7-reverse); CAG CCC CAT TCC CCT ATG TGT TTC (UGT1A8-forward) and GAG CAT CGG CGA AAT CCA TGA AT (UGT1A8-reverse). Real-time PCR analysis (model 7300; Applied Biosystems) was performed with the following PCR method: 95°C for 10 min, 40 to 45 cycles of 95°C for 30 s, and 60°C for 60 s. Specificity was verified by sequencing of representative PCR products, and in each run by PCR product duplex melting temperature analysis. Negative controls included exclusion of cDNA template and reverse transcription enzyme. mRNA concentrations were calculated by using standard curves of PCR threshold cycle number versus concentration of template derived from serial dilutions of purified PCR product. Curves were linear ($r^2 > 0.99$) over the concentration range 10^{-9} to 10^{-14} M for 18S rRNA and 10^{-14} to 10^{-18} M for other genes, defining the upper and lower quantitation limits of the respective assays. For each tissue, cDNA reactions were performed in triplicate and quantitative PCR reactions were performed at least in duplicate. Results are expressed as the mean (\pm S.E.) number of mRNA copies per 10^9 copies of 18S rRNA. Assay precision as reflected by the coefficient of variation of replicates averaged 29, 32, and 36% for UGT1A6, UGT1A7, and UGT1A8, respectively.

Results

Psilocin and Psilocin Glucuronide Stability. Stock solutions of psilocin and 4-hydroxyindole, 100 mM in methanol, appeared stable for at least 48 h, if kept at -20°C and protected from light. However, buffered aqueous solutions of psilocin (pH 7.4), particularly in the presence of proteins and at 37°C , as in the glucuronidation reactions, were unstable even for short periods of time. The degradation of psilocin, presumably due to oxidation, was first noticed from the pronounced darkening of the solution, and it was accompanied by the appearance of numerous additional peaks in the HPLC chromatogram. The presence of DMSO in the reaction mixture seemed to accelerate psilocin degradation, and, therefore, it was excluded from all the glucuronidation assays involving psilocin and 4-hydroxyindole. However, even in the absence of DMSO, psilocin degradation in the aqueous reaction mixture took place, and it was not fully prevented by protecting the samples from light. Hence, it was necessary to find a way to prevent this degradation without affecting the UGTs activity.

The effect of two reducing agents on psilocin stability and glucuronidation rates, ascorbic acid and DTT, was assayed by using UGT1A10 as the glucuronidating enzyme. Ascorbic acid prevented the observed darkening of the sample, but its addition led to the

appearance of various chromatographic peaks that interfered with the HPLC analyses (data not shown). The use of DTT, on the other hand, prevented both the visual darkening and the rise of additional peaks. Moreover, the inclusion of up to 2.5 mM DTT in the reaction mixture resulted in a clear increase in the peak area of the substrate psilocin, as well as a moderate rise in the peak area of psilocin glucuronide (Fig. 2A). At the optimal DTT concentration of 1 mM , the psilocin and psilocin glucuronide peak areas were approximately 135 and 115% of the corresponding values in the absence of DTT (Fig. 2A). DTT was not included in the 4-hydroxyindole glucuronidation assays because there was no clear need for it. However, DTT was included in the 4-hydroxyindole glucuronidation inhibition assays for consistency, because psilocin was used in part of these reactions (see below).

Possible direct effects of DTT on the catalytic activity of UGT1A10 were excluded after examination of β -estradiol glucuronidation by the enzyme. Even in the presence of high DTT concentrations, the estradiol glucuronidation results barely deviated from the glucuronidation rate in the absence of this reducing agent (Fig. 2B). Other human UGTs that catalyze psilocin glucuronidation were also tested for possible DTT effect, and, like with UGT1A10, no significant inhibition was found (data not shown). The stability of psilocin glucuronide in the supernatant fractions, after reaction termination by perchloric acid addition and the subsequent centrifugation, was also examined. Psilocin glucuronide was stable when stored at room temperature for 72 h, at least if kept in amber glass vials. Based on these results, 1 mM DTT was included in all subsequent psilocin glucuronidation assays.

Screening Recombinant UGTs and Human Microsomes for Psilocin and 4-Hydroxyindole Glucuronidation Activity. Glucuronidation of psilocin by the 19 human UGTs of subfamilies 1A, 2A, and 2B was assayed in the presence of three substrate concentrations, 100, 500, and $1000 \mu\text{M}$. None of the UGT2A or 2B subfamily

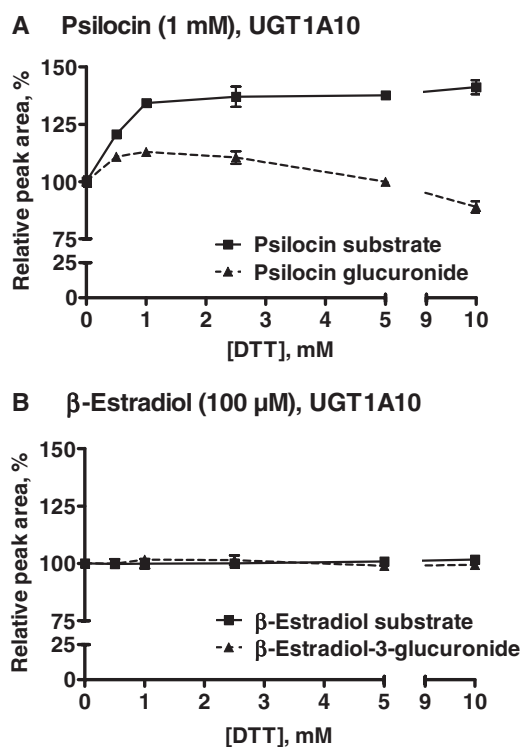


Fig. 2. Influence of DTT concentration on psilocin (A) and β -estradiol (B) glucuronidation activity by UGT1A10. The results (mean \pm S.E., $n = 3$) are presented as the relative peak area (in percent) under the curve, for both substrate and glucuronide peaks, compared with control samples without DTT.

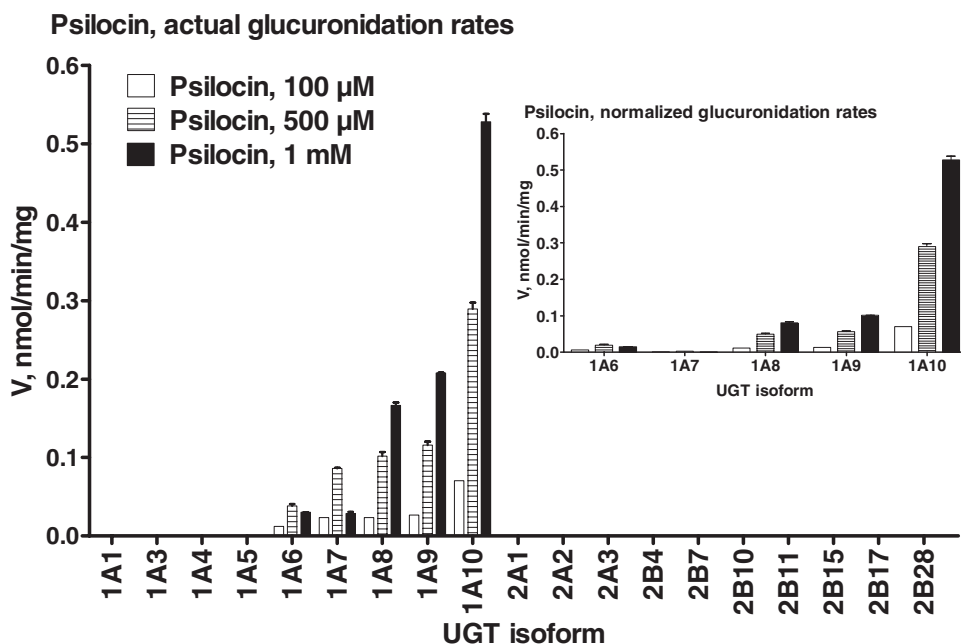


FIG. 3. Glucuronidation of psilocin by 19 human recombinant UGTs. The screening assay was performed at three psilocin concentrations (100, 500, and 1000 μM). The bars represent mean ($n = 3$) \pm S.E. The results are presented as actual glucuronidation rates (measured rates). For the active UGTs, the results are presented as normalized rates (corrected for relative expression level). The expression level of UGT1A10 was used as 1.0 for normalization. See *Materials and Methods* for additional details.

enzymes exhibited detectable psilocin glucuronidation activity. Among the nine enzymes of subfamily 1A, UGT1A10 exhibited the highest activity. Substantially lower activity was found for UGT1A9 and UGT1A8, whereas the normalized activities of UGT1A6 and, particularly, UGT1A7 were very low (Fig. 3). A parallel experiment for identifying human UGTs that catalyze 4-hydroxyindole glucuronidation was performed by using two substrate concentrations, 100 and 500 μM . The results of this screen revealed that UGT1A6 is by far the most active enzyme in 4-hydroxyindole glucuronidation (Fig. 4). Moderate activity was observed for UGT1A10, low glucuronidation rates were detected for UGT1A9, UGT1A8, and UGT2A1, while the activity of UGT1A7 was minimal (Fig. 4).

The psilocin and 4-hydroxyindole glucuronidation activity in HLM and HIM was also examined, using the same respective substrate concentrations as with the recombinant UGTs. The results showed

that whereas the psilocin glucuronidation rates in HIM and HLM are very similar (Fig. 5A), the 4-hydroxyindole glucuronidation rate in HLM is approximately 10-fold higher than the corresponding rate in HIM (Fig. 5B).

Psilocin glucuronidation reactions by all the tested samples, recombinant human UGTs as well as human liver and intestinal microsomes, yielded only one psilocin glucuronide peak. Neither the use of two different methods to stop the reaction, perchloric acid versus cold methanol addition, nor the two different chromatographic methods for psilocin glucuronide detection (see under *Materials and Methods*) resulted in the appearance or detection of a second UDPGA-dependent peak. Likewise, only one 4-hydroxyindole glucuronide was detected in all of our assays.

Enzyme Kinetics Studies. Studies on psilocin glucuronidation kinetics were performed with UGT1A10 and UGT1A9 (Fig. 6),

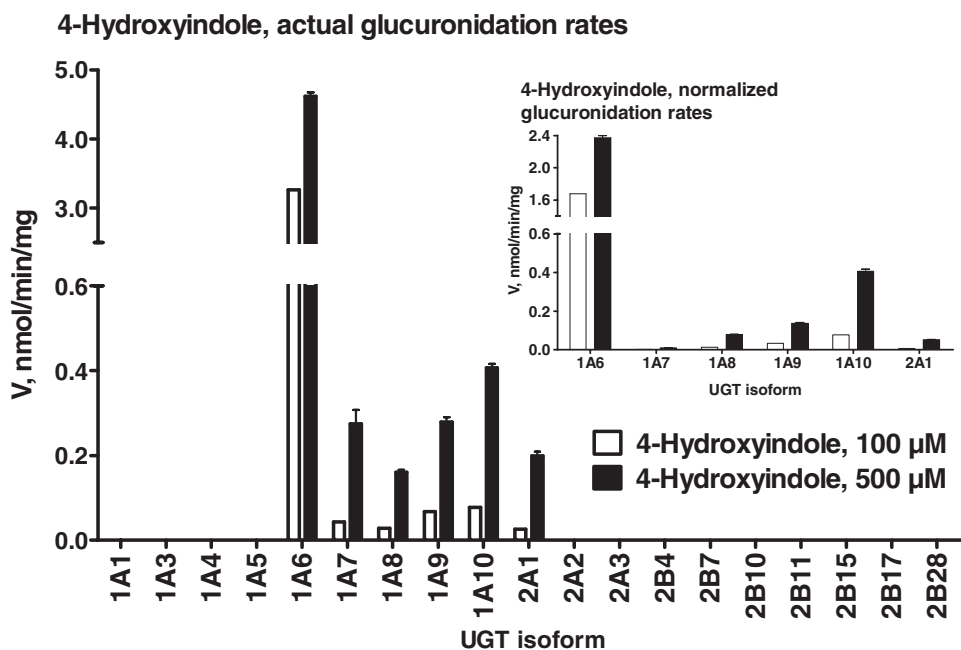


FIG. 4. Glucuronidation of 4-hydroxyindole by 19 human recombinant UGTs. The screening assay was performed at two 4-hydroxyindole concentrations (100 and 500 μM). The results are presented as both measured and normalized rates (see legend to Fig. 3).

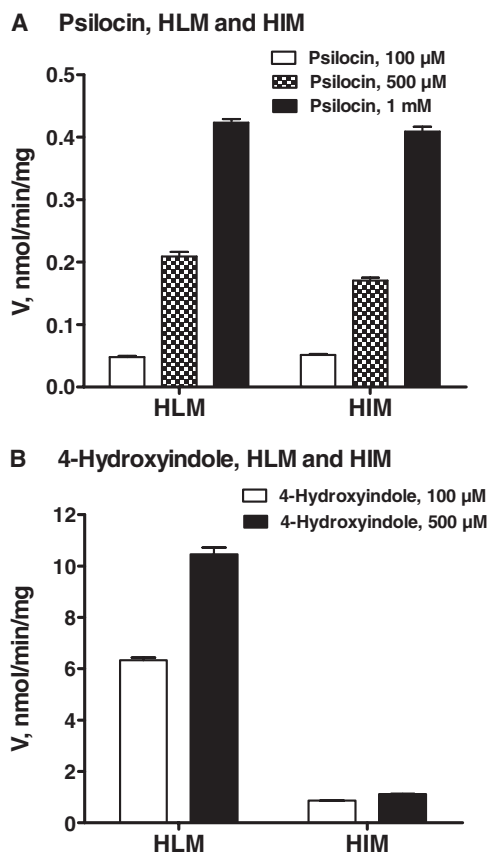


FIG. 5. Glucuronidation of psilocin (A) and 4-hydroxyindole (B) by HLM and HIM. The assays were performed at three psilocin concentrations (100, 500, and 1000 μM) and two 4-hydroxyindole concentrations (100 and 500 μM). The bars represent an average of three samples \pm S.E.

whereas the kinetics of 4-hydroxyindole glucuronidation was examined in UGT1A6, UGT1A10, and UGT2A1 (Fig. 7). Assay conditions in the kinetic reactions were optimized for the different UGT enzymes so that the glucuronidation rate was within the linear range with respect to both protein concentration and incubation time in each case. In addition, care was taken that no more than 10% of the substrate was consumed in these reactions. It may also be noted here that the number of different substrate concentration points, up to 12, was higher than in most similar studies. The data were plotted both as velocity versus substrate concentration and as velocity versus velocity divided by substrate concentration (Figs. 6 and 7, Eadie-Hofstee plots, shown as insets) to enable better selection of the appropriate kinetic model. The criteria for best model selection are described under *Materials and Methods*, and the calculated kinetic parameters are presented in Table 1.

Catalysis of psilocin glucuronidation by UGT1A10 followed hyperbolic Michaelis-Menten kinetics (Fig. 6A). The substrate affinity for the enzyme was low, as indicated by the large K_m value (over 3 mM), whereas the estimated V_{max} value was rather high (Table 1). The kinetics of psilocin glucuronidation by UGT1A9 proved difficult to resolve. The velocity of the reaction rose almost linearly with increasing psilocin concentration until the solubility limit was reached at 5 mM, rendering estimation of kinetic parameters by the Michaelis-Menten equation inaccurate. Inspection of the Eadie-Hofstee plot revealed somewhat convex curving and, thus, the possibility of biphasic kinetics. Hence, the data were fitted by using the two-site biphasic kinetic model (Korzekwa et al., 1998), which assumes the existence of two binding sites that are significantly different in sub-

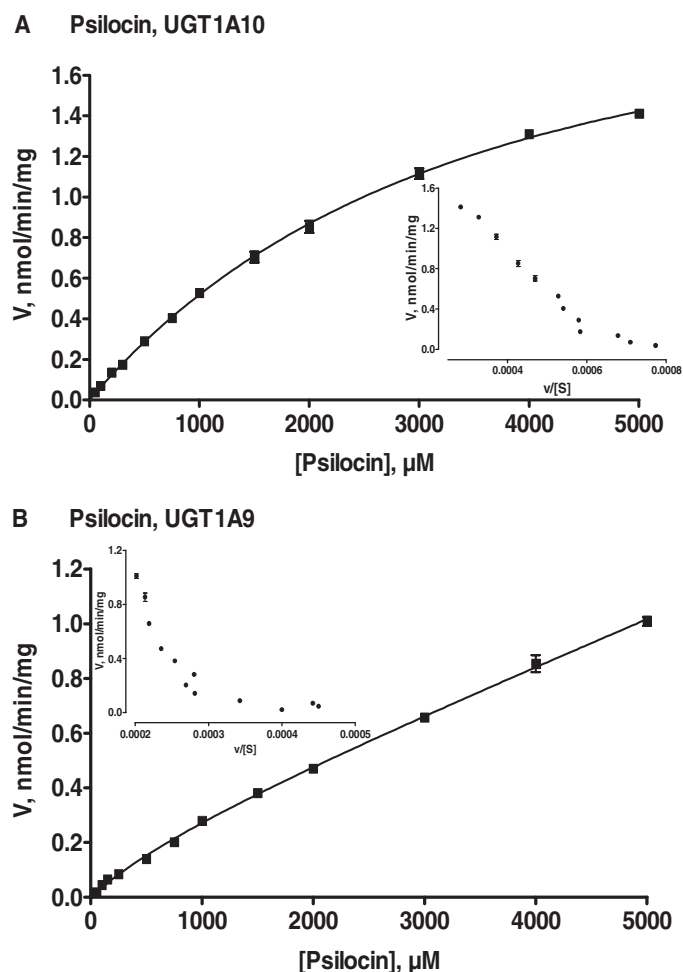


FIG. 6. Enzyme kinetics of psilocin glucuronidation by UGT1A10 (A) and UGT1A9 (B). The points represent an average of three samples \pm S.E. Glucuronidation rates are presented as actual (measured) rates in nmol/min/mg recombinant protein. The derived kinetic constants and normalized glucuronidation values are presented in Table 1. For psilocin glucuronidation by UGT1A10, the data were fitted to the Michaelis-Menten equation. For UGT1A9, data were fitted to the two-site biphasic equation. The Eadie-Hofstee transforms of the data are presented as insets.

strate affinity. The K_{m1} and V_{max1} values for the first, higher affinity site of UGT1A9 were determined from the lower portion of the curve (Fig. 6B). The upper portion of the plot was linear and no saturation was achieved, making accurate estimation of the lower affinity component K_{m2} and V_{max2} values unfeasible.

The glucuronidation of 4-hydroxyindole by UGT1A6 was characterized by pronounced substrate inhibition kinetics (Fig. 7A). UGT1A6 exhibited relatively high affinity for this substrate ($K_m < 200 \mu\text{M}$), resulting in considerable enzyme efficiency. UGT1A10, on the other hand, displayed low affinity for 4-hydroxyindole, reflected by a high K_m value ($> 3 \text{ mM}$) and high V_{max} value (approximately half the corresponding value in UGT1A6) (Fig. 7B; Table 1). Careful examination of the corresponding Eadie-Hofstee plot for 4-hydroxyindole glucuronidation by UGT1A10 suggested possible sigmoidal kinetics at the lower concentration range, 50 to 500 μM . However, the mild substrate inhibition at high concentrations of 4-hydroxyindole, 2 to 5 mM, was more obvious, and the substrate inhibition equation was thus used to derive the kinetic parameters (Table 1).

The UGT2B enzymes glucuronidated neither psilocin nor 4-hydroxyindole (Figs. 3 and 4). In addition to UGTs 1A6–1A10, the only

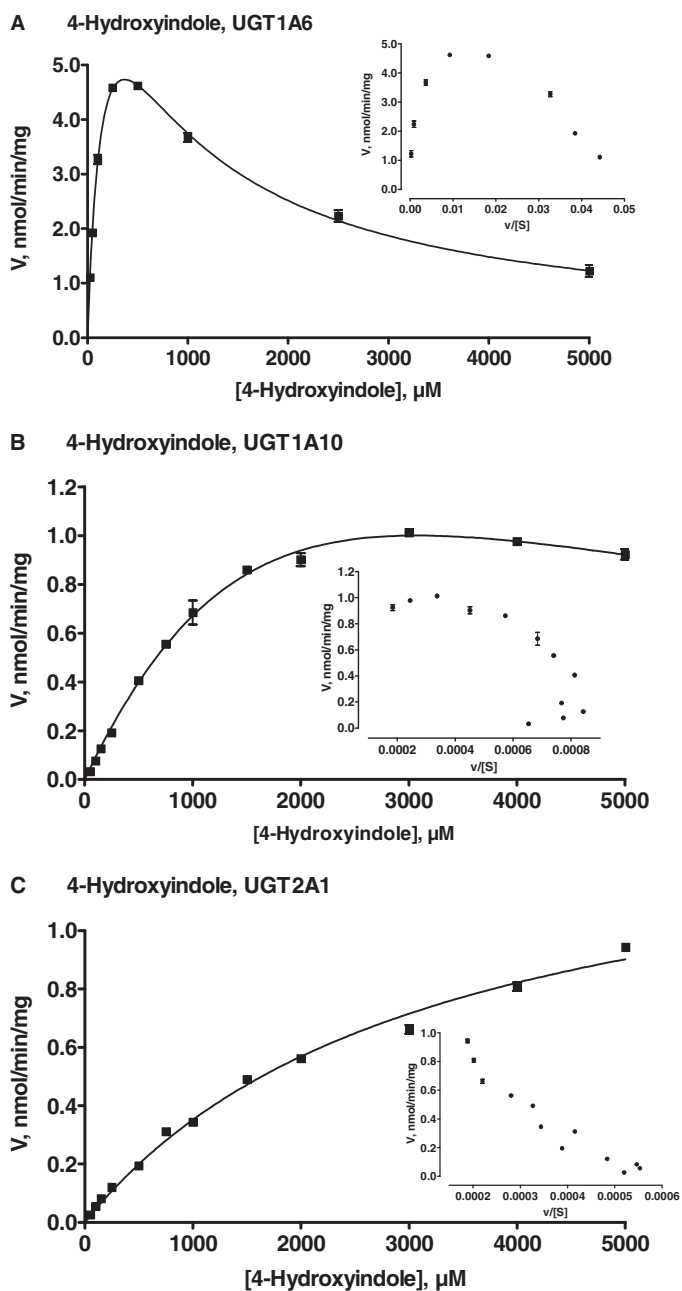


FIG. 7. Enzyme kinetics of 4-hydroxyindole glucuronidation by UGT1A6 (A), UGT1A10 (B), and UGT2A1 (C). The points represent an average of three samples \pm S.E. Glucuronidation rates are presented as actual (measured) rates in nmol/min/mg recombinant protein. The derived kinetic constants and normalized glucuronidation values are presented in Table 1. For 4-hydroxyindole glucuronidation by UGT1A6, the data were fitted to substrate inhibition equation. For 4-hydroxyindole glucuronidation by UGT1A10, the data were fitted to the substrate inhibition equation, and in the case of UGT2A1 it was fitted to the Michaelis-Menten equation. The Eadie-Hofstee transforms of the data are presented as insets.

human UGT that exhibited measurable 4-hydroxyindole glucuronidation activity was the nasal epithelium enzyme UGT2A1 (Fig. 4). The kinetics of the latter reaction was best described by the Michaelis-Menten equation (Fig. 7C) and the analysis revealed low affinity, as indicated by the high K_m value (>3 mM) and a moderate V_{max} (Table 1).

Inhibition of the UGT1A6 Catalyzed 4-Hydroxyindole Glucuronidation. One of the main findings of this study is that whereas UGT1A10 interacts with psilocin and 4-hydroxyindole similarly, UGT1A6 exhibits a large preference for 4-hydroxyindole (Figs. 3 and

4; Table 1). The negligible activity of UGT1A6 in psilocin glucuronidation could either be due to poor affinity, binding in a nonproductive way, or both. To obtain more information on this result, we have tested the efficiency of psilocin as an inhibitor of 4-hydroxyindole glucuronidation by UGT1A6. The inhibition assays were performed in the presence of 200 μ M 4-hydroxyindole, close to its K_m value for UGT1A6 (179 μ M; Table 1). The results clearly show that the inhibition by psilocin was mild and mainly visible at very high concentrations, above 2 mM (Fig. 8A). As a positive control for this inhibition study, we have tested 1-naphthol, a good substrate for UGT1A6. In sharp contrast to psilocin, 1-naphthol almost fully suppressed 4-hydroxyindole glucuronidation when added in equimolar amounts (Fig. 8B).

Quantitative mRNA Expression of the Psilocin Glucuronidating UGTs. To gain further insight into the possible locations of psilocin glucuronidation in the human body, we examined the expression level of the genes encoding UGTs 1A6–1A10 by quantitative real-time PCR (qRT-PCR). As shown in Table 2, both UGT1A6 and UGT1A9 were most highly expressed in liver, with lower but comparable levels in kidney, small intestines, and colon. Compared with UGT1A9, substantially higher UGT1A6 expression was observed in stomach and trachea, whereas UGT1A9 was much more highly expressed in liver and kidney compared with UGT1A6. UGT1A7 was most highly expressed in kidney, whereas UGT1A8 was most highly expressed in liver. Overall, UGT1A7 and UGT1A8 were expressed in much lower levels than UGT1A6 and UGT1A9 in most tissues evaluated. The only exception was the adrenal gland, which expressed more UGT1A7 compared with other UGTs. UGT1A10 was most highly expressed in small intestine and colon, and the levels of UGT1A10 in these tissues were higher than all other UGTs evaluated.

Discussion

Psilocin glucuronide is a major psilocin metabolite in humans (Sticht and Käferstein, 2000; Kamata et al., 2003, 2006), and we have now examined the glucuronidation of psilocin, as well as 4-hydroxyindole, a structural analog of psilocin that lacks the *N,N*-dimethylaminoethyl side chain of this recreational drug (Fig. 1).

Psilocin turned out to be unstable under the assay conditions, presumably due to nonenzymatic oxidation (Anastos et al., 2006). We have overcome this problem by including DTT in the reaction mixture (Fig. 2A). The inclusion of 1 mM DTT in the reaction mixture had no significant effect on the glucuronidation of β -estradiol by UGT1A10 (Fig. 2B). The latter is not in full agreement with two reports about the stimulatory effect of DTT on the glucuronidation of *p*-nitrophenol and apomorphine by rat liver microsomes (El-Bachá et al., 2000; Ikushiro et al., 2002). Nevertheless, similarly to β -estradiol glucuronidation, DTT had no obvious effect on 4-hydroxyindole glucuronidation rates (data not shown). Hence, it appears to us that DTT may be used as an efficient antioxidant for glucuronidation studies using substrates that are prone to oxidative degradation.

Both psilocin and 4-hydroxyindole have two potential glucuronidation sites (Fig. 1), but we have detected only one glucuronide. Based on studies with structurally related molecules, like serotonin (Krishnaswamy et al., 2003), 5-hydroxytryptophol (Krishnaswamy et al., 2004), 5-hydroxy-*N,N*-diisopropyltryptamine (Kamata et al., 2006), and dopamine (Itäaho et al., 2009), we can conclude with considerable confidence that human UGTs only catalyze the glucuronidation of psilocin and 4-hydroxyindole at their respective hydroxy groups. This conclusion is in agreement with the lack of detectable activity by either UGT1A4 or UGT2B10, but this observation cannot be taken as an evidence for the lack of *N*-glucuronidation.

TABLE 1

Psilocin and 4-hydroxyindole glucuronidation kinetics

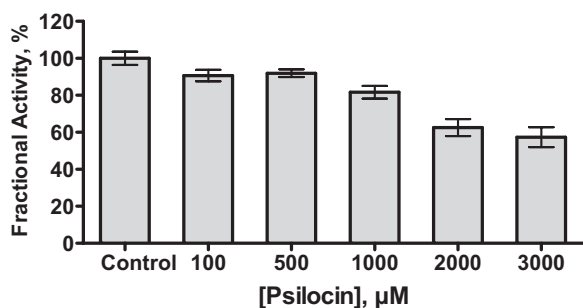
The values represent a best-fit result \pm S.E. The reaction velocity is presented both as actual rates and rates normalized to UGT1A10 expression level (i.e., for UGT1A10, the actual and normalized rates are identical). See *Materials and Methods* for additional details.

Substrate	Enzyme	K_m	V_{max} (Actual Rates)	V_{max} (Normalized Rates)	K_{is}	Kinetic Model (r^2)
		μM	$nmol/min/mg$	$nmol/min/mg$	μM	
Psilocin	UGT1A10	3851.0 ± 166.6	2.53 ± 0.06			Michaelis-Menten (0.997)
	UGT1A9	$K_{m1} = 1017.0 \pm 249.9^a$	$V_{max1} = 0.38 \pm 0.14^a$	$V_{max1} = 0.19 \pm 0.04^a$		Two-site biphasic (0.996)
4OH-Indole	UGT1A10	3624.0 ± 839.7^b	3.36 ± 0.63^b		2603.0 ± 744.8	Substrate inhibition (0.992)
	UGT1A6	178.7 ± 14.8	9.31 ± 0.45		765.1 ± 65.5	Substrate inhibition (0.991)
	UGT2A1	3210.0 ± 235.7	1.48 ± 0.06	0.39 ± 0.02		Michaelis-Menten (0.992)

^a The calculated CL_{int} is $1.69 \times 10^{-4} \pm 1.04 \times 10^{-5}$ ml/min/mg (normalized, $8.29 \times 10^{-5} \pm 5.12 \times 10^{-6}$ ml/min/mg) and represents the linear portion of the biphasic curve (ratio V_{max2}/K_{m2}). Data were also fitted to the Michaelis-Menten equation, $K_m = 12047 \pm 1428 \mu M$, $V_{max} = 3.41 \pm 0.31$ (normalized, 1.66 ± 0.15) nmol/min/mg, $r^2 = 0.996$.

^b Data were also fitted to the Hill equation, $S_{50} = 631.6 \pm 32.7 \mu M$, $V_{max} = 1.03 \pm 0.02$ nmol/min/mg, Hill coefficient $h = 1.60 \pm 0.11$, $r^2 = 0.986$.

A 4-Hydroxyindole glucuronidation by UGT1A6 in the presence of psilocin



B 4-Hydroxyindole glucuronidation by UGT1A6 in the presence of 1-naphthol

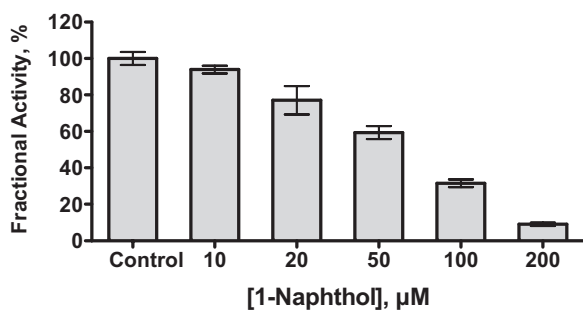


FIG. 8. Inhibition of UGT1A6-catalyzed 4-hydroxyindole glucuronidation by psilocin (A) and 1-naphthol (B). The concentration of 4-hydroxyindole was 200 μM . The glucuronidation rate of the uninhibited reaction was 5.29 ± 0.19 nmol/min/mg (mean \pm S.E.). Results are presented as percentage of activity relative to control incubations without inhibitor. Bars represent an average of three samples \pm S.E.

UGT1A10 is the most active human enzyme in psilocin glucuronidation (Fig. 3). UGTs 1A8 and 1A9 also exhibited considerable psilocin glucuronidation activity, whereas the normalized activities of UGTs 1A6 and 1A7 were very low. The pattern of psilocin glucuronidation by the different human UGTs is different from serotonin, structurally the closest compound to psilocin that has been studied thus far in this way. Although serotonin is a nearly selective substrate for UGT1A6 (Krishnaswamy et al., 2003), psilocin is glucuronidated by UGTs 1A8–1A10 at higher rates than by UGT1A6 (Fig. 3). It is worth noting here that although serotonin is almost exclusively glucuronidated by UGT1A6 (Krishnaswamy et al., 2003; Kurkela et al., 2007), serotonin is not a high-affinity substrate for UGT1A6. Because psilocin is also a low-affinity substrate for the human UGTs that glucuronidate it (see below), the difference between the two compounds from the glucuronidation point of view may not be that large after all.

The 4-hydroxyindole glucuronidation screen revealed 100-fold higher reactivity by UGT1A6 in comparison to its psilocin glucuronidation activity, whereas the activities of UGTs 1A7–1A10 were rather similar toward both substrates (Fig. 4). Serotonin is a well known specific substrate for UGT1A6, although it is worth pointing out here its low affinity for UGT1A6, namely a K_m value in the range of 5 to 6 mM (Krishnaswamy et al., 2003). In any case, the difference in UGT1A6 activity between psilocin to serotonin may arise from the size difference between them due to the more bulkier *N,N*-dimethylaminoethyl side chain of psilocin (Fig. 1). It is also possible that the spatial orientation of the psilocin hydroxy group, placed at a position 4 of the indole ring, brings it in close proximity to the conformationally flexible side chain in position 3, therefore inducing steric hindrance, which has a detrimental effect on UGT1A6 activity. This steric hindrance hypothesis is in line with the finding that 4-hydroxyindole, a structural analog of psilocin that lacks side chain, is a very good substrate for UGT1A6 (Fig. 4). Nevertheless, the inhibition studies (Fig. 8) suggest that the size difference between serotonin and psilocin may be of primary importance when binding to UGT1A6. Psilocin inhibits glucuronidation of 4-hydroxyindole by UGT1A6 only when present at a concentration that is 10- to 15-fold higher than 4-hydroxyindole, whereas 1-naphthol is efficiently inhibiting at equimolar concentrations (Fig. 8). Thus, it is tempting to suggest that the relatively bulkier side chain of psilocin prevents it from binding to the active site of UGT1A6, the somewhat smaller side chain of serotonin allows for low-affinity binding, whereas 4-hydroxyindole faces no (or much less) size limitations in its binding to UGT1A6.

Looking at the differences between psilocin and serotonin from the point of view of UGTs 1A8–1A10, one may wonder if it is the position of the OH group or the chemical nature of the side chain that is mainly responsible. It is possible that the significantly higher hydrophobicity of psilocin ($\log P = 1.45$; Migliaccio et al., 1981) in comparison with serotonin ($\log P = 0.2$; value from <http://pubchem.ncbi.nlm.nih.gov/>) plays a role in stimulating psilocin glucuronidation by UGT1A10. On the other hand, because the activities of UGTs 1A8–1A10 in 4-hydroxyindole glucuronidation (Fig. 4) are similar to their respective psilocin glucuronidation rates (Fig. 3), the presence or absence of the *N,N*-dimethylaminoethyl side chain appears to have a minor effect on the preference of UGTs 1A8–1A10 for psilocin over serotonin.

Although UGT1A10 is the most active human UGT in psilocin glucuronidation, the affinity of psilocin for this enzyme is low (Fig. 6A; Table 1). The glucuronidation of psilocin by UGT1A9 exhibited atypical kinetics (Fig. 6B) that may be best described by a two-site biphasic kinetics model in which the first binding site (could also be a subdomain within a large binding site) has higher affinity but low turnover rate, whereas the other site has very low substrate affinity

TABLE 2

Tissue-specific expression of UGTs 1A6, 1A7, 1A8, 1A9, and 1A10

The data are given as mRNA copies/10⁹ copies of 18S rRNA, mean ± S.E.

Tissue	UGT mRNA Expression in Human Tissues				
	1A6	1A7	1A8	1A9	1A10
	<i>copies/10⁹ copies of 18S rRNA, mean ± S.E.</i>				
Adipose	28 ± 8	18 ± 6	8 ± 2	86 ± 15	313 ± 57
Adrenal gland (n = 62)	3.0 ± 0.3	43 ± 9	—	3.0 ± 0.4	—
Brain	—	—	—	—	—
Brain, cerebellum (n = 24)	—	—	—	—	—
Colon (n = 3)	215 ± 22	79 ± 22	25 ± 8	188 ± 55	1210 ± 299
Kidney	226 ± 19	104 ± 12	—	2157 ± 269	—
Liver, adult (n = 47)	923 ± 9	40 ± 11	—	3239 ± 42	6.0 ± 0.2
Lung	2 ± 1	—	—	—	—
Ovary	—	—	—	—	—
Pancreas	—	—	—	—	—
Placenta	4.0 ± 0.3	3.0 ± 0.1	—	3.0 ± 0.2	—
Prostate (n = 47)	68 ± 2	9 ± 1	1 ± 1	8 ± 1	6 ± 1
Small intestine (n = 5)	334 ± 77	80 ± 33	12 ± 2	319 ± 109	660 ± 254
Stomach	184 ± 59	7 ± 1	—	4 ± 1	21 ± 3
Testis (n = 19)	14 ± 2	2.0 ± 0.3	1.0 ± 0.3	13 ± 3	6 ± 1
Thyroid (n = 65)	11 ± 1	3 ± 1	—	1.0 ± 0.1	—
Trachea	693 ± 76	26 ± 9	7.0 ± 0.5	32 ± 7	27 ± 8
Uterus (n = 10)	53 ± 13	—	—	—	—

—, not detected.

and a higher turnover rate (Fig. 6B; Table 1). Biphasic kinetics in UGT1A9 was previously described for naproxen glucuronidation (Bowalgaha et al., 2005).

The 4-hydroxyindole glucuronidation kinetics of UGT1A6 revealed high substrate affinity, considerable turnover rates, and pronounced substrate inhibition (Fig. 7A; Table 1). It may be added here that the screening results suggest that substrate inhibition also takes place in psilocin glucuronidation by UGT1A6 and UGT1A7 (Fig. 3). The high activity of UGT1A6 toward 4-hydroxyindole, as well as the results of the inhibition experiment (Fig. 8), are in agreement with the broadly accepted idea that UGT1A6 “specializes” in small and planar aromatic substrates.

Our results concerning the expression of UGTs 1A6–1A10 in a selection of tissues are generally in good agreement with a recent study that used a similar qRT-PCR method (Ohno and Nakajin, 2009). The gene expression results revealed that none of the examined UGTs, namely 1A6–1A10, is expressed in the brain (Table 2), implying that in humans neither psilocin nor serotonin is glucuronidated inside this organ. The expression level of UGT1A10 in the small intestine is more than 100-fold higher than its expression in the liver, an organ in which UGT1A9 is highly expressed (Izukawa et al., 2009; Ohno and Nakajin, 2009) (Table 2).

The differential expression of UGTs 1A9 and 1A10, in combination with the screening and kinetics results for psilocin glucuronidation (Figs. 3 and 6), can well explain our finding that the psilocin glucuronidation rate in HIM, per milligram of microsomal protein, is very similar to the rate in HLM (Fig. 5A). In the case of 4-hydroxyindole, the glucuronidation rate in HLM was approximately 10-fold higher than in HIM (Fig. 5B). The qRT-PCR results, together with the kinetics of 4-hydroxyindole glucuronidation by UGT1A6, suggest that most of the 4-hydroxyindole glucuronidation activity in both HLM and HIM is due to UGT1A6 activity. However, some contribution of UGT1A9 to 4-hydroxyindole glucuronidation in the liver cannot be excluded.

In this study we have examined the glucuronidation of psilocin by the human UGTs of subfamilies 1A, 2A, and 2B. UGT1A10 is the most active enzyme in psilocin glucuronidation, but UGT1A9, due to its high expression in the liver, may be the main contributor to psilocin

glucuronidation in man. Alongside psilocin, we have analyzed the glucuronidation of 4-hydroxyindole, a structurally related indole, and found that UGT1A6 plays a major role in its glucuronidation. These results shed new light on the substrate selectivity of the human UGTs and suggest new directions in this complex research field.

Acknowledgments. We thank Johanna Mosorin for skillful technical assistance and Antti Siiskonen for valuable advices regarding chemistry. Qin Hao and Dr. Leah Hesse are acknowledged for their role in generating the UGT mRNA quantitation data.

References

- Anastos N, Barnett NW, Pfeffer FM, and Lewis SW (2006) Investigation into the temporal stability of aqueous standard solutions of psilocin and psilocybin using high performance liquid chromatography. *Sci Justice* **46**:91–96.
- Bjornstad K, Hulten P, Beck O, and Helander A (2009) Bioanalytical and clinical evaluation of 103 suspected cases of intoxications with psychoactive plant materials. *Clin Toxicol (Phila)* **47**:566–572.
- Bowalgaha K, Elliot DJ, Mackenzie PI, Knights KM, Swedmark S, and Miners JO (2005) S-Naproxen and desmethylnaproxen glucuronidation by human liver microsomes and recombinant human UDP-glucuronosyltransferases (UGT): role of UGT2B7 in the elimination of naproxen. *Br J Clin Pharmacol* **60**:423–433.
- El-Bachá RS, Leclerc S, Netter P, Magdalou J, and Minn A (2000) Glucuronidation of apomorphine. *Life Sci* **67**:1735–1745.
- Fisher MB, Campanale K, Ackermann BL, VandenBranden M, and Wrighton SA (2000) In vitro glucuronidation using human liver microsomes and the pore-forming peptide alamethicin. *Drug Metab Dispos* **28**:560–566.
- González-Maeso J, Weisstaub NV, Zhou M, Chan P, Ivic L, Ang R, Lira A, Bradley-Moore M, Ge Y, Zhou Q, Sealton SC, and Gingrich JA (2007) Hallucinogens recruit specific cortical 5-HT(2A) receptor-mediated signaling pathways to affect behavior. *Neuron* **53**:439–452.
- Grieshaber AF, Moore KA, and Levine B (2001) The detection of psilocin in human urine. *J Forensic Sci* **46**:627–630.
- Halpern JH (2004) Hallucinogens and dissociative agents naturally growing in the United States. *Pharmacol Ther* **102**:131–138.
- Hasler F, Bourquin D, Brenneisen R, and Vollenweider FX (2002) Renal excretion profiles of psilocin following oral administration of psilocybin: a controlled study in man. *J Pharm Biomed Anal* **30**:331–339.
- Hasler F, Bourquin D, Brenneisen R, Bär T, and Vollenweider FX (1997) Determination of psilocin and 4-hydroxyindole-3-acetic acid in plasma by HPLC-ECD and pharmacokinetic profiles of oral and intravenous psilocybin in man. *Pharm Acta Helv* **72**:175–184.
- Holzmann PP (1995) *Bestimmung van Psilocybin-Metaboliten im Human Plasma and Urin*. Ph.D. thesis, Eberhard-Karls-Universität, Tübingen, Germany.
- Ikushiro S, Emi Y, and Iyanagi T (2002) Activation of glucuronidation through reduction of a disulfide bond in rat UDP-glucuronosyltransferase 1A6. *Biochemistry* **41**:12813–12820.
- Itäaho K, Court MH, Uutela P, Kostianen R, Radomska-Pandya A, and Finel M (2009) Dopamine is a low-affinity and high-specificity substrate for the human UDP-glucuronosyltransferase 1A10. *Drug Metab Dispos* **37**:768–775.
- Itäaho K, Mackenzie PI, Ikushiro S, Miners JO, and Finel M (2008) The configuration of the 17-hydroxy group variably influences the glucuronidation of beta-estradiol and epiestradiol by human UDP-glucuronosyltransferases. *Drug Metab Dispos* **36**:2307–2315.
- Izukawa T, Nakajima M, Fujiwara R, Yamanaka H, Fukami T, Takamiya M, Aoki Y, Ikushiro

- S, Sakaki T, and Yokoi T (2009) Quantitative analysis of UDP-glucuronosyltransferase (UGT) 1A and UGT2B expression levels in human livers. *Drug Metab Dispos* **37**:1759–1768.
- Kaivosaarinen S, Toivonen P, Aitio O, Sipilä J, Koskinen M, Salonen JS, and Finel M (2008) Region- and stereospecific N-glucuronidation of medetomidine: the differences between UDP glucuronosyltransferase (UGT) 1A4 and UGT2B10 account for the complex kinetics of human liver microsomes. *Drug Metab Dispos* **36**:1529–1537.
- Kamata T, Katagi M, Kamata HT, Miki A, Shima N, Zaitu K, Nishikawa M, Tanaka E, Honda K, and Tsuchihashi H (2006) Metabolism of the psychotomimetic tryptamine derivative 5-methoxy-N,N-diisopropyltryptamine in humans: identification and quantification of its urinary metabolites. *Drug Metab Dispos* **34**:281–287.
- Kamata T, Nishikawa M, Katagi M, and Tsuchihashi H (2006) Direct detection of serum psilocin glucuronide by LC/MS and LC/MS/MS: time-courses of total and free (unconjugated) psilocin concentrations in serum specimens of a “magic mushroom” user. *Forensic Toxicol* **24**:36–40.
- Kamata T, Nishikawa M, Katagi M, and Tsuchihashi H (2003) Optimized glucuronide hydrolysis for the detection of psilocin in human urine samples. *J Chromatogr B Analyt Technol Biomed Life Sci* **796**:421–427.
- King CD, Rios GR, Green MD, and Tephly TR (2000) UDP-glucuronosyltransferases. *Curr Drug Metab* **1**:143–161.
- Korzekwa KR, Krishnamachary N, Shou M, Ogai A, Parise RA, Rettie AE, Gonzalez FJ, and Tracy TS (1998) Evaluation of atypical cytochrome P450 kinetics with two-substrate models: evidence that multiple substrates can simultaneously bind to cytochrome P450 active sites. *Biochemistry* **37**:4137–4147.
- Krishnaswamy S, Duan SX, Von Moltke LL, Greenblatt DJ, and Court MH (2003) Validation of serotonin (5-hydroxytryptamine) as an in vitro substrate probe for human UDP-glucuronosyltransferase (UGT) 1A6. *Drug Metab Dispos* **31**:133–139.
- Krishnaswamy S, Hao Q, Von Moltke LL, Greenblatt DJ, and Court MH (2004) Evaluation of 5-hydroxytryptophol and other endogenous serotonin (5-hydroxytryptamine) analogs as substrates for UDP-glucuronosyltransferase 1A6. *Drug Metab Dispos* **32**:862–869.
- Kurkela M, Patana AS, Mackenzie PI, Court MH, Tate CG, Hirvonen J, Goldman A, and Finel M (2007) Interactions with other human UDP-glucuronosyltransferases attenuate the consequences of the Y485D mutation on the activity and substrate affinity of UGT1A6. *Pharmacogenet Genomics* **17**:115–126.
- Mackenzie PI, Bock KW, Burchell B, Guillemette C, Ikushiro S, Iyanagi T, Miners JO, Owens IS, and Nebert DW (2005) Nomenclature update for the mammalian UDP glycosyltransferase (UGT) gene superfamily. *Pharmacogenet Genomics* **15**:677–685.
- Migliaccio GP, Shieh TL, Byrn SR, Hathaway BA, and Nichols DE (1981) Comparison of solution conformational preferences for the hallucinogens bufotenin and psilocin using 360-MHz proton NMR spectroscopy. *J Med Chem* **24**:206–209.
- Nakamura A, Nakajima M, Yamanaka H, Fujiwara R, and Yokoi T (2008) Expression of UGT1A and UGT2B mRNA in human normal tissues and various cell lines. *Drug Metab Dispos* **36**:1461–1464.
- Ohno S and Nakajin S (2009) Determination of mRNA expression of human UDP-glucuronosyltransferases and application for localization in various human tissues by real-time reverse transcriptase-polymerase chain reaction. *Drug Metab Dispos* **37**:32–40.
- Shirota O, Hakamata W, and Goda Y (2003) Concise large-scale synthesis of psilocin and psilocybin, principal hallucinogenic constituents of “magic mushroom.” *J Nat Prod* **66**:885–887.
- Sneitz N, Court MH, Zhang X, Laajanen K, Yee KK, Dalton P, Ding X, and Finel M (2009) Human UDP-glucuronosyltransferase UGT2A2: cDNA construction, expression, and functional characterization in comparison with UGT2A1 and UGT2A. *Pharmacogenet Genomics*.
- Stamets P (2003) *Psilocybin Mushrooms of the World: An Identification Guide*, 1st edition ed. Ten Speed Press.
- Sticht G and Käferstein H (2000) Detection of psilocin in body fluids. *Forensic Sci Int* **113**:403–407.
- Tsujikawa K, Kanamori T, Iwata Y, Ohmae Y, Sugita R, Inoue H, and Kishi T (2003) Morphological and chemical analysis of magic mushrooms in Japan. *Forensic Sci Int* **138**:85–90.
- Tukey RH and Strassburg CP (2000) Human UDP-glucuronosyltransferases: metabolism, expression, and disease. *Annu Rev Pharmacol Toxicol* **40**:581–616.
- Turgeon D, Carrier JS, Lévesque E, Hum DW, and Bélanger A (2001) Relative enzymatic activity, protein stability, and tissue distribution of human steroid-metabolizing UGT2B subfamily members. *Endocrinology* **142**:778–787.

Address correspondence to: Dr. Moshe Finel, CDR, Faculty of Pharmacy, P.O. Box 56 (Viikinkaari 5 E), University of Helsinki, FI-00014 Helsinki, Finland. E-mail: Moshe.Finel@helsinki.fi
